STAG: Smart Tools and Applications in Graphics (2020)
S. Biasotti, R. Pintus and S. Berretti (Editors)

Smart Modelling of Geologic Stratigraphy Concepts using Sketches

M. Costa Sousa,[1†] J.D. Machado Silva,[1†] C.C.M. Machado Silva,[1‡] F.M. De Carvalho,[1§] S. Judice,[1†] F. Rahman,[1†] C. Jacquemyn,[2¶] M.E.H. Pataki,[2‡] G.J. Hampson,[2‡] M.D. Jackson,[2‡] D. Petrovskyy[3‖] and S. Geiger[3§]

[1]Department of Computer Science, University of Calgary, Canada
[2]Department of Earth Science & Engineering, Imperial College London, UK
[3]School of Energy, Geoscience, Infrastructure and Society, Heriot-Watt University, UK

Abstract

Several applications of Earth Science require geologically valid interpretation and visualization of complex physical structures in data-poor subsurface environments. Hand-drawn sketches and illustrations are standard practices used by domain experts for conceptualizing their observations and interpretations. These conceptual geo-sketches provide rich visual references for exploring uncertainties and helping users formulate ideas, suggest possible solutions, and make critical decisions affecting the various stages in geoscience studies and modelling workflows. In this paper, we present a sketch-based interfaces and modelling (SBIM) approach for the rapid conceptual construction of stratigraphic surfaces, which are common to most geologic modelling scales, studies, and workflows. Our SBIM approach mirrors the way domain users produce geo-sketches and uses them to construct 3D geologic models, enforcing algorithmic rules to ensure geologically-sound stratigraphic relationships are generated, and supporting different scales of geology being observed and interpreted. Results are presented for two case studies demonstrating the flexibility and broad applicability of our rule-based SBIM approach for conceptual stratigraphy.

CCS Concepts

•***Applied computing*** → ***Earth and atmospheric sciences;***

1. Introduction

Several important socio-economic applications of Earth Science, including hydrocarbon exploration, geothermal energy utilization, groundwater resources management, and storage in deep geological repositories (e.g., carbon dioxide and nuclear waste) are multi-disciplinary problems requiring geologically valid interpretation and visualization of complex physical structures in data-poor subsurface environments. Geological models are typically the first ones to be developed in this context thus impacting the complete subsurface study and modelling workflow. Modelling geological structures, however, is very challenging. These structures are often invisible to the naked eye, presenting different geometries and properties that need to be captured in 3D at multiple scales (i.e., from nanometer to kilometer). Subsurface data availability is also insufficient, collected at sparse locations, with limited depth range, and in different modalities and resolutions (e.g., seismic, core samples), presenting varying degrees of uncertainty primarily due to natural variability (i.e., the heterogeneity of geological structures) [BF04, NHRT07].

In order to explore these uncertainties, in particular during the early stages of geological studies and modelling, users build a range of conceptual models, commonly represented in the form of hand-drawn sketches and illustrations [BGSJ07,RBLM19,Com17]. These traditional geo-sketches (Figure 1) represent conceptualizations based on laboratory and field observations and interpretations of geological formations visible on the surface (e.g., outcrop analogues) [Com17] from acquired datasets (e.g. seismic surveys, photogrammetry, well-logs) [Vai87], and for scientific illustration, discussions and dissemination of geologic concepts [GCO*17, Hod03, YCF10]. Conceptual geo-sketches provide rich visual references for exploring uncertainties and helping users formulate ideas, suggest possible solutions, and make critical decisions that affect subsequent stages of geoscience studies and modelling workflows [Hod03, GUS*14, Rob15]. One critical limitation in current geo-modelling workflow (e.g., [Can18, Mal02]) is the limited number of computational tools and mathematical approaches allowing users to interactively construct conceptual digital surface-based geo-models seamlessly and rapidly from hand-drawn, conceptual geo-sketches. Many computational tools proposed to aid the user in this process have their foundations in the field of sketch-

† {smcosta,machadoj,sicilia.judice,fazilatur.rahman}@ucalgary.ca
‡ Currently at Computer Modelling Group Ltd., Canada, clarissa.silva@cmgl.ca
§ Currently at the Tecgraf Institute of Technical-Scientific Software Development of PUC-Rio (Tecgraf/PUC-Rio), Brazil, felipemc@tecgraf.puc-rio.br
¶ {c.jacquemyn,m.pataki,g.j.hampson,m.d.jackson}@imperial.ac.uk
‖ {d.petrovskyy,S.Geiger}@hw.ac.uk

DOI: 10.2312/stag.20201243

based interfaces and modelling (SBIM) [JS11, OSCSJ09]. This field introduced a new paradigm that leverages our natural drawing skills, allowing us to build 3D models more intuitively and to gain new insights into exploring their 3D architecture and uncertainties. SBIM techniques should 'mimic' the way domain experts produce sketches, enforcing geological rules (to ensure geologically-sound models are generated), and supporting different scales of geology being observed and interpreted. Conceptual sketch-based geomodelling algorithms and methods would complement approaches currently used for generating digital geo-models, by providing a more interpretive geo-model representation – i.e., the resulting conceptual, sketch-based geo-model would directly convey the observations and interpretations depicted in the hand-drawn, conceptual digital geo-sketches.

In this paper, we present a rule-based SBIM system with a set of generic, universally applicable operators, to define how stratigraphic surfaces must interact to produce geologically sound sketch-based models. The integrated use of generic operators is a novel development that distinguishes our work from previous SBIM applications to geology; it allows users to sketch viable models in a quick and geologically intuitive manner. We demonstrate that models created with our system honour fundamental stratigraphic and sedimentologic concepts such as the law of superposition, Walther's Law, sequence stratigraphy, and facies models (e.g., [WB99, JYMJ05, CCLCdV*09]).

Stratigraphy is a branch of geology that deals with the formation, composition, sequence, and correlation of stratified rocks and sediments (i.e., natural material broken down by weathering and erosion, and transported by wind, water, ice or gravity). Stratigraphic surfaces define the boundaries and internal subdivisions of successions of sedimentary rocks and enclose discrete geometric bodies of sediment. We chose to investigate and develop the functionality to model stratigraphy for two primary reasons. First, most geologic modelling scales contain stratigraphic surfaces, but not all modelling scales contain faults and other structural geological features. Second, faults are planar discontinuities across which stratigraphic surfaces are displaced. Thus, stratigraphy must be modelled in order to define the displacement across a fault.

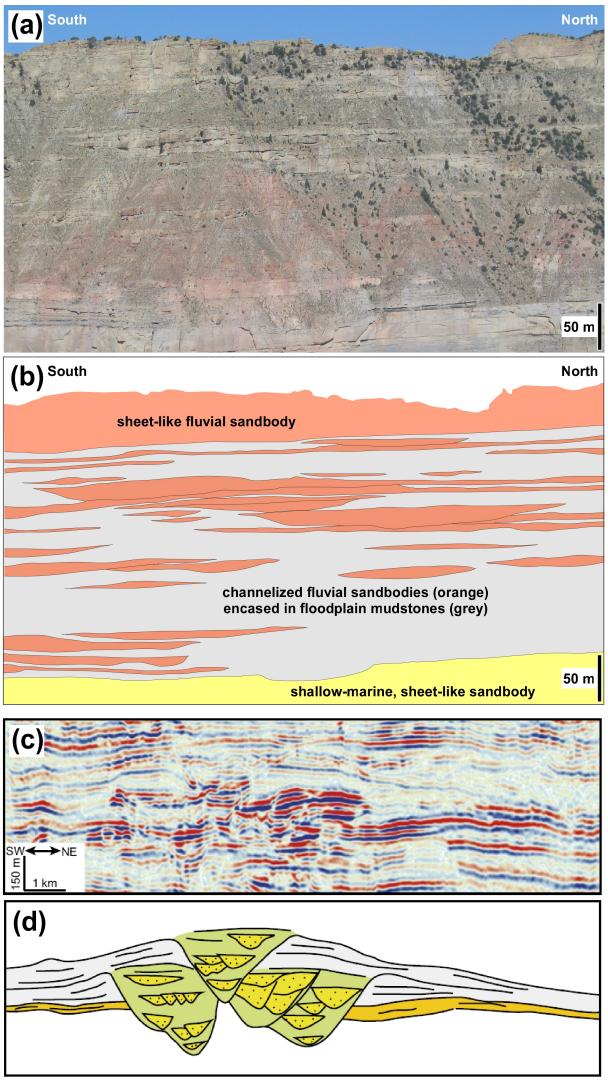

Figure 1: *Examples of hand-drawn concept sketches of interpretive geology.* ***(a)*** *An outcrop analogue for subsurface geological modelling studies and its* ***(b)*** *interpretive sketch depicting exposed sandbody geometries and distributions. Figures in (a, b) modified from Figure 3 in Villamizar et al. [VHFF15].* ***(c)*** *Seismic cross-section and its* ***(d)*** *interpretive sketch depicting nested channelized geobodies. Figures in (c, d) from [MFS*20].*

2. Related work

2.1. Concept-driven SBIM

Research in concept-driven SBIM has been receiving increasing attention. A fundamental challenge is to approximate surfaces from construction lines with varying degrees of uncertainty about the geometry and topology of the intended form being conceptualized. Related works propose fundamental algorithms and techniques to process those uncertainties to build and augment forms represented as planar or free-form surfaces – e.g., [AOK12, GJ12, NISA07, OSD06] - with demonstration examples for industrial design (e.g., [BBS08, OK12, SBSS12]), character design (e.g., [DPS15]), developable materials (e.g., [JHR*15b]), botany (e.g., [IYYI14, APCS09]), terrain modelling (e.g., [GGP*19, NLP*13]), and in geology as described in the next subsection.

2.2. SBIM for geology

An early work on SBIM for geology is from Schild *et al.* [SHB09]. They propose a SBIM virtual reality system for seismic volume annotation and segmentation. Seismic volumes are also used by Amorim *et al.* [AVBPCS12] with a SBIM system for post-processing pre-extracted seismic horizons and interactive modelling of new ones. The user sketches over slices from a seismic volume, with sketch-based operators for geometry adjustment and topology repair. In their approach, the input sketches are constrained to seismic reflections.

Multi-touch tabletop SBIM approaches have also been proposed for collaborative conceptual modelling of geological formations. Amorim *et al.* [ABVB*12] presents a SBIM system where the user sketches directly over point cloud data from microseismic events for reconstructing a triangulated volume approximating the Stimulated Reservoir Volume (SRV). Sultanum *et al.* [SVBCS13] propose a system for collaborative visual exploration, extraction and reconstruction of conceptual surfaces from LiDAR-based outcrop analogues. Amorim *et al.* [AVBSCS14] propose a multi-touch, mobile SBIM system for 3D modelling of bedding dip and strike, folds, and faults. The user sketches in a blank-screen (i.e., no data), in plan view (a.k.a. map view), the geometries, symbols and numerical input describing geological contacts and structures (dip and strike, folds, faults) inspired by traditional plan view illustrations and maps. Their approach integrates algorithmic rules to produce geologically-sound rock layered models. These rules include (1) geological contacts must not self-intersect; (2) contacts always define closed regions on a map; (3) a rock layer cannot be adjacent to itself; and (4) a specific rock layer can exist only in one series (i.e. subdivisions of rock layers based on the age of the rock).

SBIM approaches have been proposed for early-stage geological modelling for describing and conceptualizing geological processes across different geologic time periods [LHV12, LNP*13]. The user sketches over a blank screen as well as over scans of traditional paper-based geological storyboards and digital seismic slices. These sketches include annotation using geometric primitives, labelling and highlighting areas on seismic sections. Additional functionalities include animating geological sketches, comparing animations to identify the most plausible geological model, synthesizing 3D models from the input sketches and texturing the stratigraphic layers.

Lidal *et al.* [LPB*13] presents a comparative study of approaches for modelling stratigraphic layers and related features. The user sketches over box-shaped and surface proxy-geometries. Natali *et al.* [NVP12, NLP*13] present a system where the user sketches over blank-screen for 3D illustrative layer-cake modelling of folding, faulting, and guided texturing between stratigraphic layers. A layer-cake model is also used by Natali *et al.* [NPP14] for rapid SBIM of 3D interactive geological illustrations of stratigraphic relationships (deposition and erosion) and folding. The approach was later extended for faults and compaction by Natali *et al.* 2014 [NKP14].

In 2015, we introduced the *Rapid Reservoir Modelling* (RRM) framework (i.e., [JHR*15a]), allowing the user to prototype a variety of geologic *concepts* using SBIM technology integrated with techniques for calculating static and dynamic reservoir behaviour (i.e., [ZGR*18,ZGR*17b,ZGR*17a]). In Jackson *et al.* [JHR*15a], we presented a high-level overview of the main components of the RRM framework with examples of conceptual SBIM for geologic maps (i.e., [AVBSCS14]) and discussions on how different geologic model concepts impact static and dynamic reservoir properties. The work described in this paper is the core SBIM component of the RRM framework for rule-based modelling of geologic stratigraphy.

Hu *et al.* [HCW16] present an automatic sketch-based stochastic subsurface reconstruction. Sketch samples are automatically generated over input seismic data and integrated with stochastic algorithms (e.g., [JHS*13]) for modelling of geo-surfaces. Their approach applies geological laws to guide the automatic sketch extraction.

Garcia *et al.* [GCR*18] present a SBIM approach integrating interactive storytelling techniques with physical simulation for generating geological cross-sections storyboards associated with different stages in the geological restoration process.

More recently, three works report SBIM approaches processing seismic volumes. Liu *et al.* [LSC*19] propose a SBIM and visualization system for interactive interpretation of stratigraphic slices extracted and processed from raw seismic volume and well data. Ferreira *et al.* [FNOV20] propose a SBIM approach for synthetic seismic images for generating realistic seismic data for communicating ideas, searching for similar structures, and supporting the creation of training data sets for supervised machine learning algorithms. Motta *et al.* [MGR19, MMGR20] present a SBIM system for modelling salt bodies. The input sketch deforms the surface of a pre-existing mesh embedded in the seismic volume, closely related to the approach proposed by Amorim *et al.* [AVBPCS12].

2.3. Rule-based geological sketching and modelling

Physical geological surfaces represent natural discontinuities such as erosion, hiatuses in deposition, faulting or intrusion. A conceptual geological SBIM system involves not only surfaces fitting the user-input construction lines, but also geologically correct relationships between the interfaces of the various geometric components being modelled. For this purpose, algorithmic construction rules and constraints need to be integrated with SBIM techniques to ensure geologically valid relationships and structures are being generated during the sketch input and in the modelling output. Previous works on SBIM for geology integrate algorithmic rules (refer to Section 2, e.g., [AVBPCS12, AVBSCS14, HCW16]).

3. SBIM system overview

3.1. Interface at a glance

Our sketching interface and modelling workflow is illustrated in Figure 2 (Left). Sketching happens in the 2D canvasses, Figure 2(d)-2(f), where a user is able to add background images such as outcrops, seismic data, well logs or previously interpreted data to guide sketching. Because it is common for subsurface reservoirs to be much wider than tall, both front-view and lateral-view windows also support having their height (z-axis) re-scaled on the fly, so that an expert may vertically exaggerate the sketching canvas to avoid clutter and to facilitate sketching thin features. Such vertical exaggerations are augmented with a dip angle (i.e., the steepest angle of descent of a tilted bed or feature relative to a horizontal plane) guiding tool, which allows the expert to know how angles between stratigraphic surfaces change as the Z-scale of the geometry changes.

Surfaces can be sketched in multiple modes, see Figure 2(b), such as in front-view cross-sections (i.e., cross-sections cutting the model alongside its *Width*), lateral-view cross-sections (*Length*), or as plan view (*Height*) contour maps. Combinations of these modes

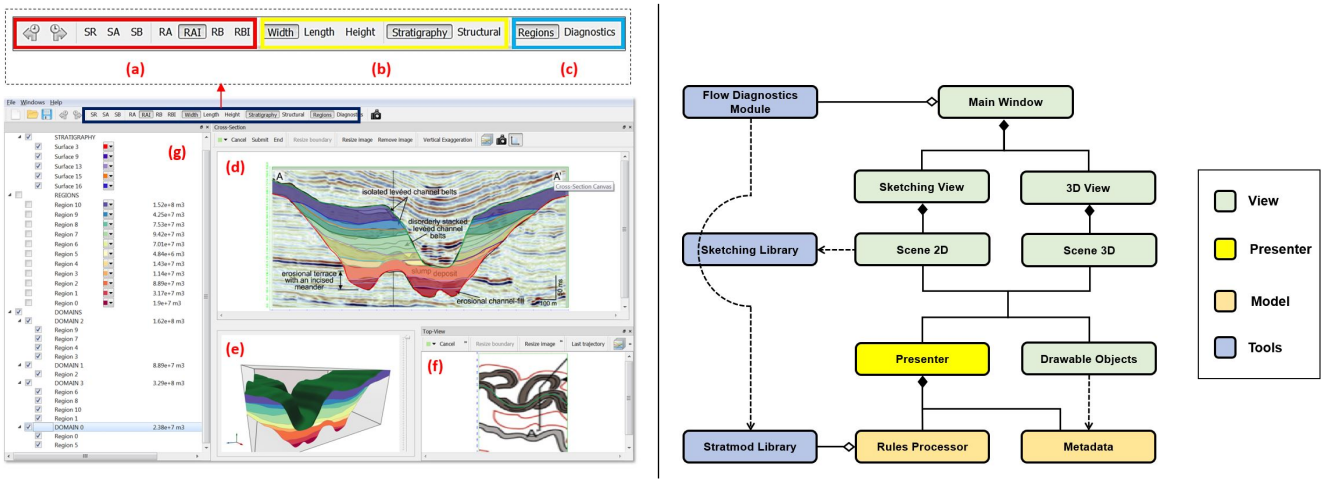

Figure 2: *(Left) Our sketching interface.* ***(a)*** *Geological operators.* ***(b)*** *Surface's creation controls.* ***(c)*** *Model introspection and diagnostics. (d) Front-view sketching plane (e.g., sketch over seismic slice from [JNHW13]) (e) 3D view. (f) plan view sketching plane. (g) Model metadata displayed in an object tree. Users can sketch in (d) and (f) to create geologic surfaces. (Right) A condensed view of our Model–View–Presenter (MVP) system architecture and independent tools (in blue).*

are also possible, such as in guided extrusions whose cross-section is sketched in front-view and the extrusion path is sketched in plan view, see Section 5.1. Our current system allows the creation of both stratigraphic and (a significant subset of) structural surfaces. Once a surface has been sketched, it is inserted in the model according to the selected geologic operator, Figure 2(a), see also Section 4. The modelling library provides undo/redo at the surface creation level to facilitate the exploration of the model design space. Models can be saved, reloaded, and modified by additional sketches.

Model introspection can be accessed through the GUI at any time, Figure 2(c). Sketched surfaces are ordered according to their relative age, and regions (i.e., volumes determined by their bounding surfaces) are automatically computed and ordered (e.g., to validate the sketched model by comparing raw volumes computed from regions to the expected rock volumes obtained from field data). Domain experts can also perform *flow diagnostics* to gather insight into the *dynamic* behaviour of the model (i.e., numerical experiments that yield quantitative information about flow dynamics in a geologic model). This aspect of our system is not reported in this manuscript, as we focus on describing the use of SBIM for building the *static* geological model. We refer the reader to the following manuscripts [ZGR*18, ZGR*17b, ZGR*17a] where we report our preliminary experiments with flow diagnostics.

Our system also allows experts to augment the models with metadata, Figure 2(g). Surfaces can be annotated with names and descriptions that explain their design. Regions can be joined in geologic domains (i.e., distinct layers of rock according to their intended geophysical properties) and named according to the type of rock they represent. All distinct objects can be colour-coded at will by the expert. Both metadata and models can be saved into files that include the full modelling session (up to the current undo/redo stack) as a means to create multiple cases from a base scenario and to document the key ideas behind the design of a particular model.

3.2. Architecture design

Our sketching architecture is illustrated with a variation of the Model-View-Presenter (MVP) pattern in Figure 2 (Right). The presenter mediates user interaction and modelling, bridging distinct software components to allow independent development of subsystems. A 2D scene handles all user interaction for sketching while sketching algorithms (smoothing, resampling, filtering, ranking, etc.) are abstracted in a general sketching library. Similarly, 3D rendering and interaction are handled by our OpenGL based subsystem. A unified collection of drawable elements can be directly accessed from the specialized 2D and 3D subsystems, thus, both input and render calls can be standardized across the whole system, allowing each specialized subsystems to focus on their specific user interactions.

A distinct subsystem handles metadata, from input data to surfaces' information, the aggregation of regions into geologic domains, and all semantic information derived from model creation. This metadata is readily available for all drawable objects, thus ensuring that it is consistently rendered in both the 2D and 3D subsystems.

Sketching and modelling are separated by a `RulesProcessor` component that bridges the main interface from the modelling tools provided by our `Stratmod` library (which implements the geologic operators, see Section 4). Our system also includes a subsystem for performing flow diagnostics (Figure 2 (Right)).

4. Logical operators for interactions of stratigraphic surfaces

4.1. Fundamental geological rules for surface interactions

To create a set of operators that apply to all types of stratigraphic surfaces, there are three geological rules which must not be violated in order to the resulting models to be geologically consistent

(Figure 3) (e.g. [WB99, JYMJ05, CCLCdV*09]). If these geological rules are obeyed, then the resulting model will contain only watertight volumes and will be geologically possible.

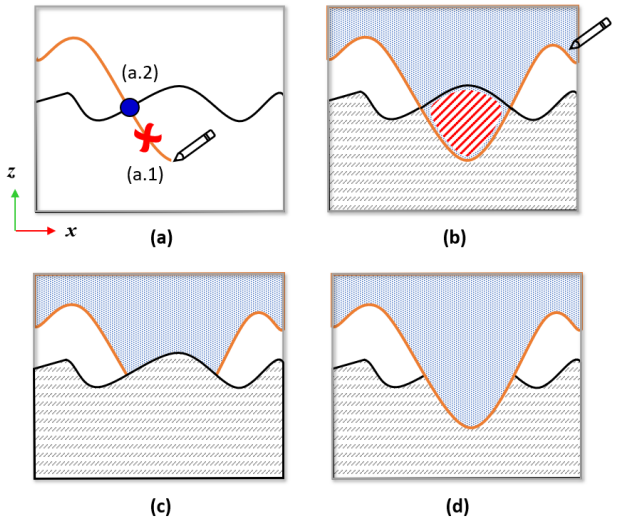

Figure 3: *Fundamental geological rules for stratigraphic surface interactions (after Caumon et al. [CCLCdV*09]). (a) Surfaces that do not terminate against an existing surface - i.e., hanging surfaces (a.1, red cross) - are cropped back to the intersection point (a.2, blue circle). (b) Surfaces that cross, defining overlapping geologic domains (i.e., distinct regions or subregions with similar structural properties), are invalid (red hatched area). Surfaces that (c) terminate at an existing surface or (d) remove an existing surface are valid.*

(1) Surfaces cannot end within a domain. Stratigraphic surfaces bound closed, watertight volumes that define *geologic domains* (i.e., distinct regions or subregions with similar internal properties). Therefore, stratigraphic surfaces cannot end within a domain (*hanging* surfaces), because this would not create a proper volumes (Figure 3a) and the same domain would exist on both sides of one surface [WB99]. The surface ending within a domain must be cropped so that it truncates against the bounding surfaces of the domain.

(2) Surfaces cannot cross. Stratigraphic surfaces are not allowed to cross because crossing surfaces create an overlapping volume that belongs simultaneously to two geologic domains (Figure 3b). Only one geologic domain can exist in any given location. To prevent two stratigraphic surfaces from crossing, one of the surfaces is modified: it is split into sub-segments delineated by the intersection line(s) created where the surfaces cross, and the unwanted surface parts are removed as necessary. The proposed operators define which of the surfaces is split and which unwanted surface parts are removed.

(3) Surfaces can either terminate against (truncate or conform) or remove (i.e., erode), existing surfaces. The proposed operators specify which of these two actions is applied. A stratigraphic surface may terminate at or remove an existing surface (Figure 3c,d).

The operators presented in this section enable that surfaces can be created in any order, so a full geologic interpretation is not required at the outset of modelling. The operators are applicable to any depositional setting. Furthermore, the operators are scale-independent, so the same operators apply whether modelling stratigraphy at different geological scales (i.e., nanometers to kilometers). A video of the operators being used to create a variety of geometric stratal configurations using our prototype SBIM system is provided in the supplemental material (Supplemental Material, Video 1).

4.2. Existing and newly created surfaces

When sketching new surfaces, there are two cases that we must consider: (1) a newly created surface is modified or constrained by existing surfaces, and (2) a new surface modifies existing surfaces. The operators enable the stratigraphic surfaces to interact such that the geologic integrity of the model is preserved in either case. In the following descriptions, the new surface is described as *n*. It is assumed that a model boundary exists, and all surfaces terminate at this boundary. In the proposed SBIM approach, the selected operator is applied immediately after each surface has been sketched and before the next surface is added. Application of the operators to a given surface as it is created is a critical aspect of our SBIM workflow.

4.3. The concept of surfaces "above" and "below"

In the operators presented in subsections 4.4 and 4.5 for stratigraphic surfaces, "above" and "below" are defined by the Cartesian coordinates (x,y,z where z represents height) of the surfaces in question at any point. We define that z is positive upwards. Points, lines and surfaces that are 'above' have a higher z-value at a given (x,y) location than the reference surface; those that are 'below' have a lower z-value than the reference surface (e.g., Figures 3 and 4. Stratigraphic surfaces are typically non-multivalued, such that they do not recur in a vertical column unless deformed by later folding and faulting. Representing the effects of such structural deformation is beyond the scope of this paper, but is the subject of ongoing research.

In the next two subsections 4.4 and 4.5, we describe how the geologic operators presented herein intuitively work. A precise definition of the geologic operators and the mathematical details concerning their properties and algorithmic implementation will be reported in future manuscripts.

4.4. Operators that modify a new surface

The following three operators describe how a new surface *n* is modified if it interacts with existing surfaces (Figure 4 (Left)).

(1) Sketch Above - SA, refer to Figure 4 (Left) (a). The SA operator preserves all parts of new surface *n* - i.e., sketching curve 4, in orange (*sc4* = '*n*,' for new) that lie above one or more selected surfaces. In the figure, the selected surface is the sketching curve *sc2* (in blue). These selected surfaces form a lower boundary for the new surface *n*.

(2) Sketch Below - SB, refer to Figure 4 (Left) (b). The SB operator

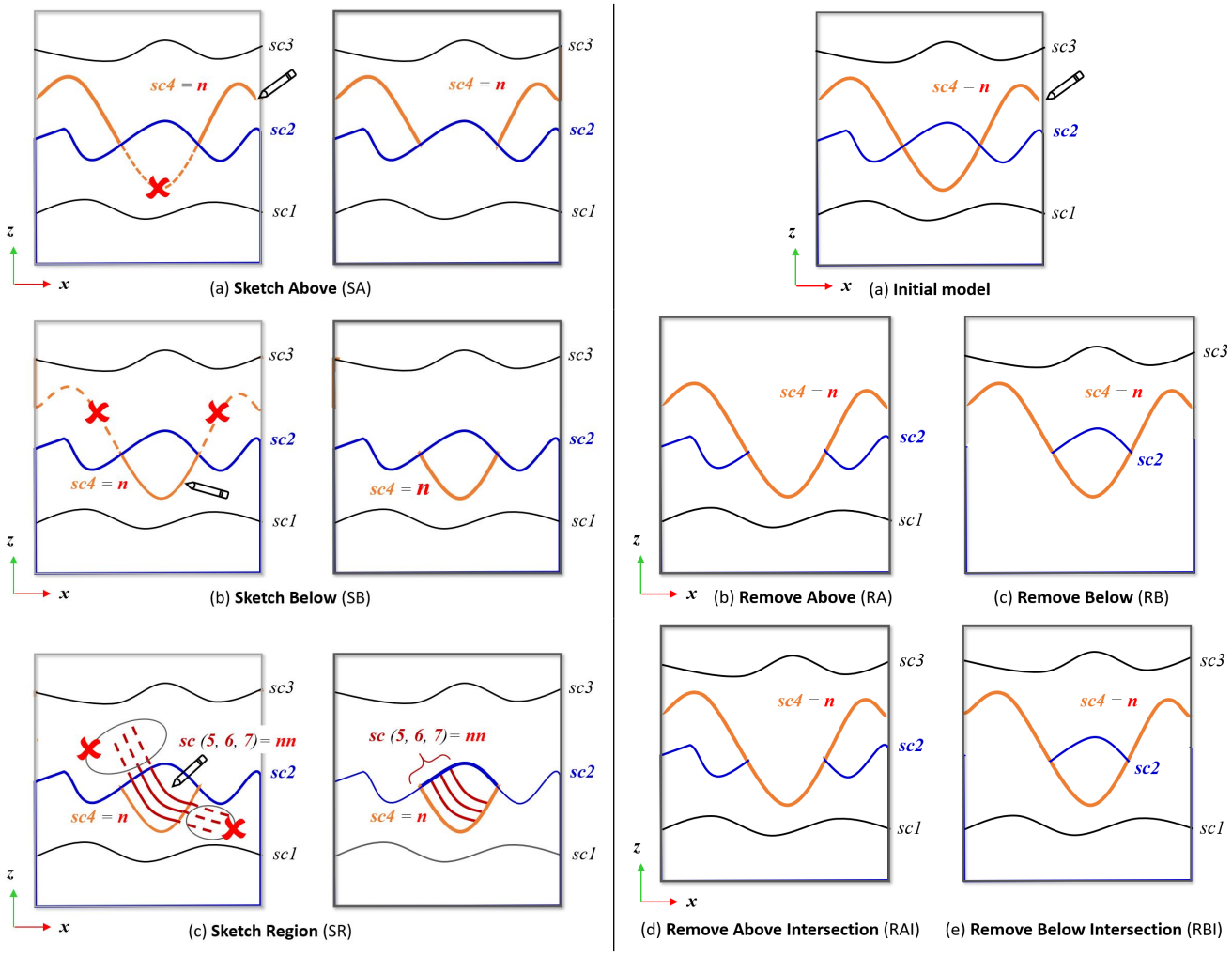

Figure 4: *Logical geo-operators modifying a new surface (Left) and an existing surface (Right).*

preserves all parts of the new surface *n* (i.e., *sc4* in orange) that lie below one or more selected surfaces (i.e., *sc2* in blue). The selected surfaces form an upper boundary for the new surface *n*.

(3) Sketch Region - SR, refer to Figure 4 (Left) (c) The SR operator is a combination of the SA and SB operators. By clicking anywhere in the sketching canvas, the SR operator automatically selects the upper and lower boundaries that define the region containing the picked position. In the figure, this area indicated by three sketched solid lines) is formed by *sc2* (in blue) and the previously sketched curve *sc4* (i.e., in orange, after applying the SB operator). Parts of any new surface *n* that are outside of the defined volume are removed. In the figure, parts of three newly sketched curves *sc5*, *sc6*, and *sc7* (in red, = '*nn*') are preserved.

4.5. Operators that modify an existing surface

The following four operators describe how existing surfaces are modified by sketching a new surface *n*, as shown in Figure 4 (Right) (a).

(1) Remove Above – RA, refer to Figure 4 (Right) (b). The RA operator removes the parts of any existing surfaces (e.g., sc3, in black and part of sc2, in blue) that lie above new surface *n* (sc4 = 'n', in orange). Existing surfaces below new surface *n* (e.g., sc1 in black) remain unchanged.

(2) Remove Below – RB, refer to Figure 4 (Right) (c). The RB operator (i.e., opposite of RA) removes the parts of any existing surfaces (e.g., sc1, in black and part of sc2, in blue) that lie below the new surface *n* (sc4 = 'n,' in orange). Existing surfaces above the new surface *n* remain unchanged (e.g., sc1 in black).

(3) Remove Above Intersection – RAI, refer to Figure 4 (Right) (d). The RAI operator removes the parts of any existing surfaces that are intersected by and lie above new surface *sc2 = 'n'* (e.g., part of sc2, in blue, is removed). Existing surfaces above and below the new surface *n* remain unchanged (e.g., sc1 in black).

(4) Remove Below Intersection - RBI, refer to Figure 4 (Right) (e). The RBI operator (i.e., opposite of RAI) removes the parts of any existing surfaces that are intersected by and lie below new sur-

face *sc2 = 'n'* (e.g., parts of sc2, in blue, are removed). Existing surfaces above and below the new surface *n* remain unchanged (e.g., sc3 in black).

5. Algorithmic creation of 3D surfaces and models

5.1. Surface interpolation

Sketches are sparse, scattered input data that are interpolated using thin-plate splines ([Duc77]) as kernels for surface reconstruction. In the case a 3D surface is built from multiple sketches (e.g., Figure 5 (a)), thin-plate spline interpolation produces the surface that minimizes a functional similar to the linear part of the surface's bending energy (e.g., Figure 5 (b)). Overfitting is avoided by reconstructing surfaces using approximate interpolation [WR05], which preserves the minimizing property of thin-plate splines while allowing interpolated surfaces to differ from input sketches within a prescribed margin of error. The balance between accuracy and stability in surface reconstruction is mediated by the resolution of the model being built and the nature of the geologic feature a 3D surface is meant to represent. The input sketches can theoretically be in any cross-section (vertical, horizontal or arbitrary). Currently, the user can sketch surfaces as profile curves in front-view (e.g., Section 6.1, Figure 7), in lateral-view cross-sections, and as depth contours in plan view (e.g., Section 6.2, Figure 10).

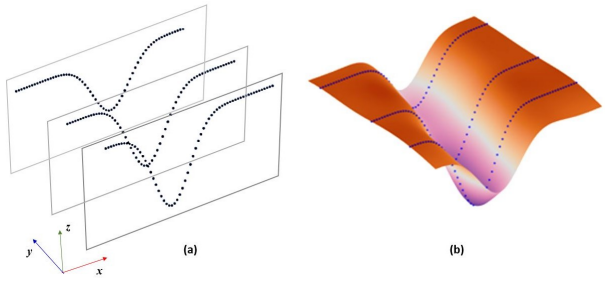

Figure 5: *Interpolation for reconstructing surfaces after the input sketches.* ***(a)*** *Sample points along the sketched curves on three front-view cross-sectional planes.* ***(b)*** *Surface after interpolating the sample points.*

Surfaces built to mimic how a cross-section curve would be extruded along a path are treated differently. If a cross-section can be extruded along with the guiding (sketched) path without incurring any self-intersections, then an actual extrusion is computed by interpolating the cross-section curve C and the path P independently and creating a surface given as a tensorial product of the input curves as follows. The height of the surface at a given point p inside the model is the height of the cross-section curve C at the point p^* in its defining cross-section, such that p^* and p can be joined by the path P. Intuitively, the cross-section curve C is carried downstream by the path P (e.g., Figure 6 (a-d)). All models presented in this manuscript were built from surfaces created with these two approaches (i.e., interpolation and guided extrusion).

5.2. Enforcing consistency with geological operators

The modelling framework enforces geometric consistency, as defined by the geologic rules in Section 2.3, by applying the operators on the interpolated surfaces. To achieve the necessary efficiency required for the rapid prototyping of geologic models, this framework processes the surfaces into a cached data structure that is amenable to computing surface intersections and performing additional queries (such as ordering the surfaces according to the relative geologic age defined by surface interactions) – time complexity scales linearly with the number of surfaces in the model, for a given mesh resolution. Our modeling system is designed to be independent of any specific mesh representation.

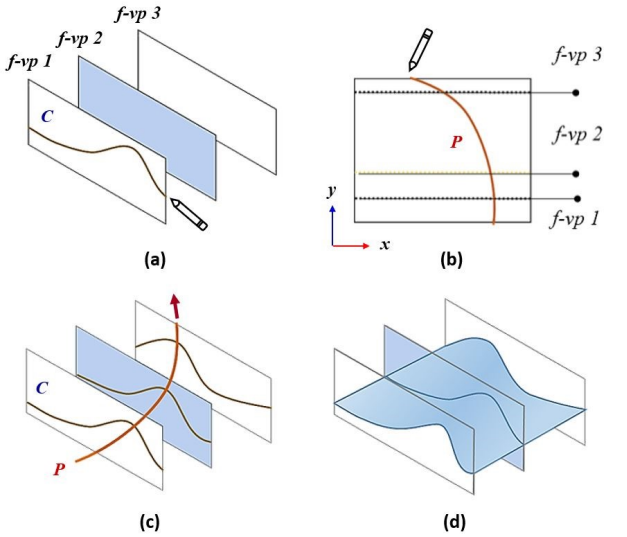

Figure 6: *Cross-section curve along a path.* ***(a)*** *Input sketch curve C in one cross-sectional font-view plane (i.e., $f-vp1$);* ***(b)*** *Path P sketched in plan view;* ***(c)*** *two snapshots of the cross-section curve carried along with the path P; and* ***(d)*** *the resulting surface after interpolating sample points from the input curves and path P.* ***Note:*** *the path P in (b) can also be sketched before the cross-section curve C.*

6. Application example results

This section demonstrates the application of the stratigraphic surface operators to two geologic cases of different length scales and deposition of sediments, using different types of data to constrain and guide sketches and different approaches to 3D surface reconstruction. Additional geological case-studies and detailed analysis involving stratigraphy as well as structures (i.e., faults) will be reported in future manuscripts.

6.1. Seismic-scale conceptual models of deepwater channel deposits

The aim of using SBIM in this first study is to prototype a plausible 3D conceptual model of channel complexes (e.g., [MPS*11]) from three parallel 2D seismic cross-sections through deepwater deposits (Figure 7) following the conceptual geological interpretation of Ma *et al.* [MFS*20] (e.g., Figure 1(d)). Channels are formed, both on land and offshore, when currents erode into underlying rocks and transport or redistribute sediments. A channel

complex is a stacked arrangement of channels (e.g., Figure 1(d)). We use our SBIM approach to construct different conceptual models to explore the uncertainty in the correlation of individual channel complexes between the seismic cross-sections.

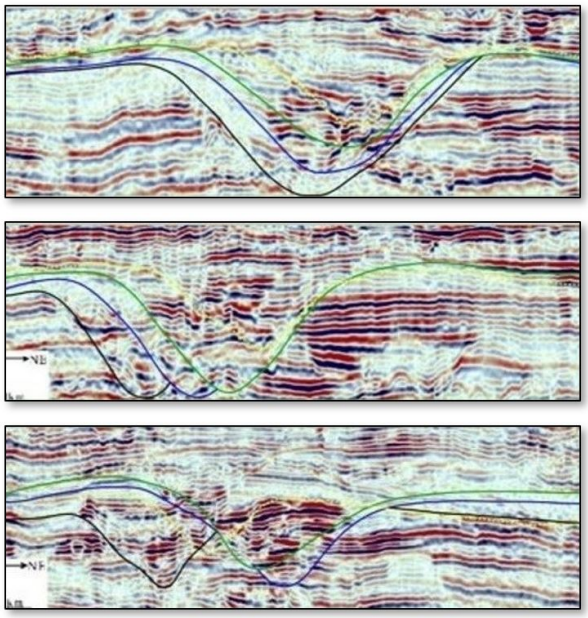

Figure 7: *Illustration of the sketch input for model construction from parallel seismic cross-sections of deepwater deposits (Section 6.1). The seismic cross-sections (from [MFS*20]) are loaded into our system. Each seismic cross-section has dimensions of 400 m (height) by 10 km (width), and the spacing between cross-sections is 14-19 km. Base surfaces of channel complexes are interpreted and modified on each cross-section, sketching from base to top surfaces using the operator RAI. Four-channel complex base surfaces are sketched. The resulting 3D model (i.e., Figure 8) honours the seismic cross-section data. A video of the prototyping is shown in Supplemental Material Video 2.*

We make an initial prototype model based on the interpretation of Ma *et al.* [MFS*20], which consists of four stacked channel complexes. We use the published seismic cross-sections as a basis on which to build our prototype model. We sketch the base surface of the lowermost channel complex, which extends across the seismic images (brown sketched surface in Figure 7) and the resulting 3D model (Figure 8). We then sketch on parallel cross-sections the construction curves representing the base surfaces of other channel complexes (blue, green and yellow sketched surfaces in Figure 7; Supplemental Material, Video 2). We interpret the interactions between surfaces representing stratigraphically *older* (i.e., early deposition of sediments) and *younger* channel complexes (i.e., more recent deposition of sediments) using the Remove Above Intersection (RAI) operator (Section 4.5). This operator prevents overlapping surfaces by removing any segments of existing surfaces that lie above a new surface (e.g., Figure 4 (Right)(d)), in this example, effectively simulating erosion. In approximately 2 minutes, we create a prototype model of Ma *et al.* [MFS*20] interpretation of the correlation between the seismic cross-sections (Figure 8A). Using the same approach, we can prototype multiple scenarios for how the channel complexes are correlated, with an alternative prototype model shown in Figure 8B. Note the interpolation of the channel-complex base surfaces between sparse cross-sections (i.e., Section 5) results in low sinuosity plan view geometries for the channel complexes (Figure 8), which is consistent with conceptual models and examples of such geological features (e.g. [MC06, MPS*11]).

The operators can be applied at multiple scale levels; therefore, we can use the same operators to add stratigraphic detail to the internal architecture within individual channel complexes (Figure 9(a, b)); Supplemental Material, Video 3). We select the individual channel complex we would like to interpret using the operator SR to define the volume we sketch within. We then use the RA operator to sketch surfaces representing the tops and bases of individual channel *elements* (i.e., bounding surfaces) [MPS*11] within the volume of the channel complex (Figure 9(a)). With the operator RB or RBI, we also insert a surface representing the top of a mass-transport deposit above the base surface of the channel complex, underlying the channel elements (Figure 9(b); Supplemental Material, Video 3).

With the method described here, combining SBIM and logical operators, it is quick and easy to prototype a range of interpretations by varying the correlation of the base surfaces of channel complexes in between the different cross-sections (Figure 8), or by creating multiple different interpretations of the internal architecture of each channel complex (Figure 9; Supplemental Material, Video 3). The user can quickly create a range of prototype models to test different correlation concepts of channel complexes between seismic cross-sections. Additionally, the user can modify the prototype model out of stratigraphic order, for example, to add internal details within channel complexes or sketch the upper (youngest) channel complex first and the underlying (older) complexes later.

6.2. Comparative outcrop-derived conceptual models of lacustrine carbonates

The aim of SBIM in this second case-study is to create two 3D prototype conceptual models that correspond to two contrasting hand-drawn interpretations of a conceptual core sample section through lacustrine carbonates (e.g., [PW09]), after Bohacs *et al.* [BLWD*13] (i.e., Figure 10(b) *left* for Interpretation A and (b) *right* for Interpretation B).

The term *lacustrine* relates to an environment of deposition in lakes, or an area having lakes. *Carbonate rocks* result from the accumulation of fossils (i.e., bioclasts) created by calcareous organisms (e.g., corals, mollusks, and algae). These lacustrine carbonates are characterized by mound-like accumulations constructed by microbes (i.e., *microbial bioherms*), comparable in scale to modern colonial corals and with a wide variety of geometries, and by carbonate sands (i.e., grainstones) (Figure 10(a)).

For this case-study, we differentiate between grainstones (i.e. made up of coarse-grained carbonate sediment) and microbial bioherms (i.e. carbonate rock accumulated under influence of microbial action). In a vertical borehole, they appear interbedded, however, laterally uncertainty exists on how they extend. Instead, con-

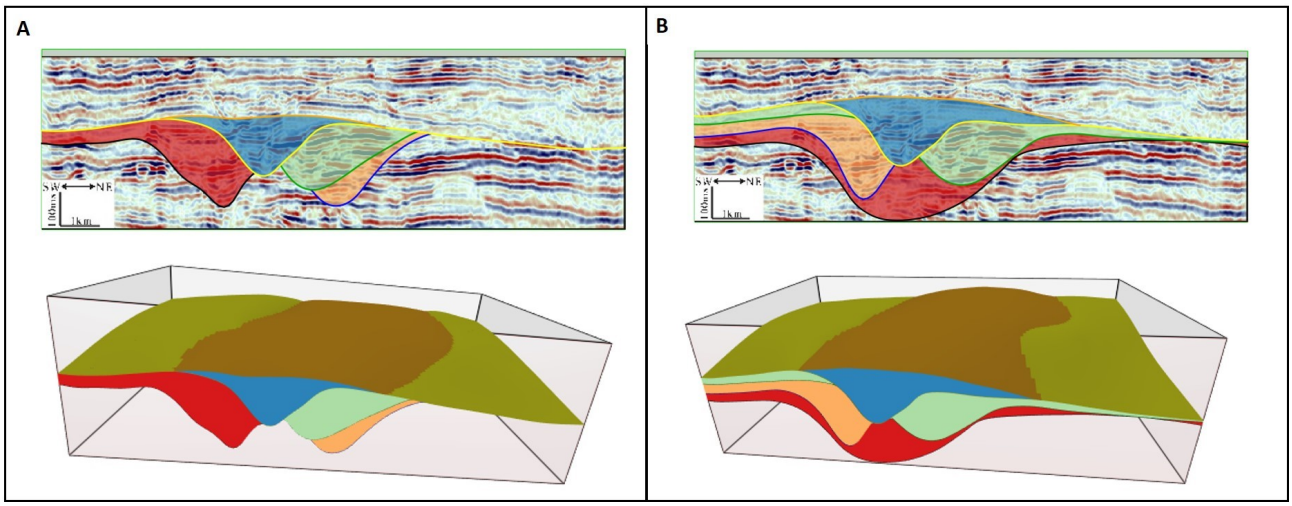

Figure 8: *Illustration of the prototype model construction from parallel seismic cross-sections of deepwater deposits [MFS*20]. In **A**, we show the result of the modelling process from Figure 7 using a seismic cross-section. This interpretation is the one shown by Ma et al. [MFS*20]. In **B**, we show an alternative prototype model of the base surfaces of channel complexes. These alternative models were made in minutes and can be used to test different geologic concepts and correlations.*

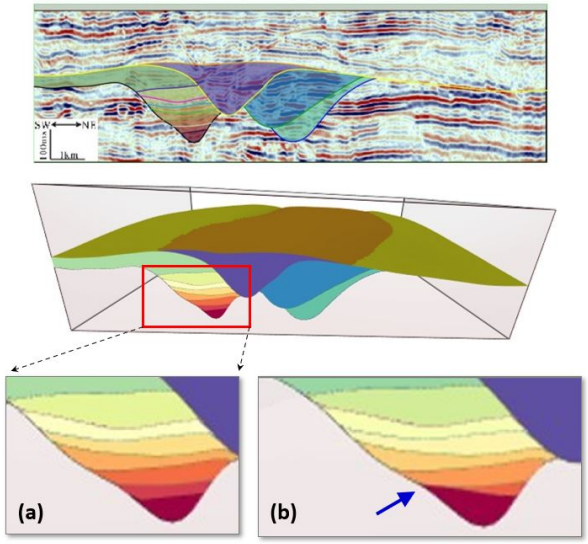

Figure 9: *Illustration of updates to the prototype model constructed and shown in Figure 8. This model is modified by adding additional architectural detail to the lowermost channel complex (zoomed-in window). Using the operator SR, we select the lowermost channel complex and add top and base surfaces of channel elements (i.e., bounding **(a)**). Then, using the operator RB, we add a mass-transport deposit top surface in the lower part of the channel complex, as indicated by the blue arrow **(b)**. The same technique could be applied to other channel complexes in the model or other prototypes of the correlation. A video of the sketching is shown in Supplemental Material Video 3.*

ceptual understanding of their internal geometrical structure must be derived by conducting interpretive studies (i.e., Figure 10(b)) of ancient examples observed in outcrops (i.e., rocks visible on the surface) analogous to the actual microbial bioherms. Outcrop analogues are interpreted by direct field observations or by studying data acquired via LiDAR or photogrammetry.

The 3D sketch-based models are generated by combining surfaces sketched on 2D vertical cross-sections (i.e., as in the first application example result in Section 6.1) with surfaces sketched as depth contours in plan view.

The prototype model of *Interpretation A* (i.e., Figure 10(c)) consists of surfaces that bound laterally continuous, sheet-like intervals, and therefore the prototype model can be made simply by extrapolating sub-parallel, non-intersecting surfaces sketched in any order on a 2D vertical cross-section (Figure 10(c); Supplemental Material, Video 4).

The prototype model of *Interpretation B* (i.e., Figure 10(d)) is made by sketching contours in plan view to create the surfaces that represent individual microbialite bioherms, confined within each stratigraphic surface layer by using the operator Sketch Region (SR) (Figure 10(b); Supplemental Material, Video 4). Starting with the surfaces sketched in Interpretation A, we select the region to sketch within (operator SR); this region represents the stratigraphic interval within which a group of microbialite bioherm were developed at the same time. One set of small circles, representing a horizontal cross-section through the microbialite bioherm mound bases, are sketched on a horizontal surface at the lower bound of the model volume (Figure 10(c); Supplemental Material, Video 4). A second set of larger circles surrounding the smaller set, representing a horizontal cross-section through the microbialite bioherm tops, are sketched on a horizontal surface at the upper bound of the model volume (Figure 10(c); Supplemental Material, Video 4). Be-

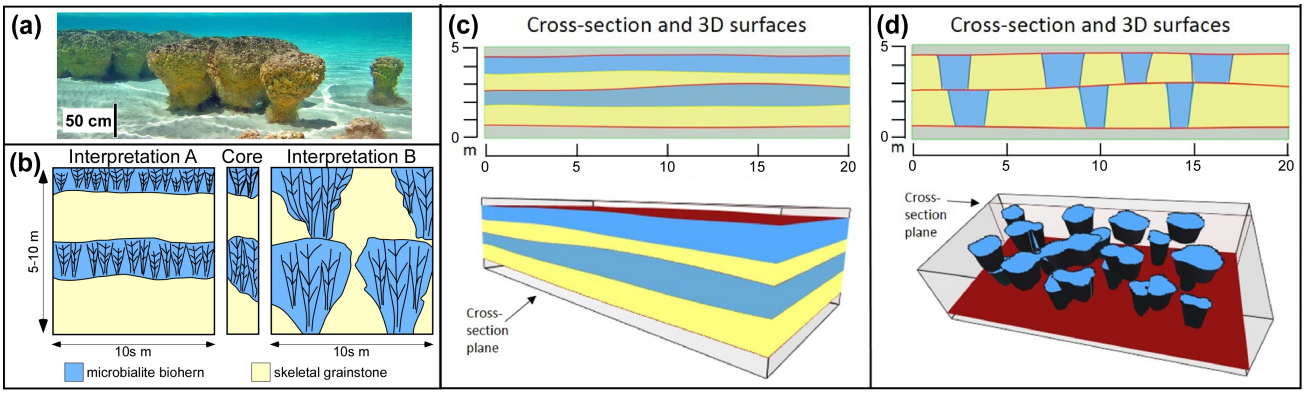

Figure 10: *Illustration of models representing expert Interpretations A and B for lacustrine microbialite and grainstone carbonates.* ***(a)****. Photograph of modern microbial bioherms (https://www.sharkbay.org/place/hamelin-pool/), showing different deposits. Some outcrop photographs showng these features can be found in [BLWD*13]) (e.g. figure 9 or 10).* ***(b)*** *Concept sketches for Interpretation A (Left) comprising continuous layers of grainstones and densely spaced microbialite bioherms, and Interpretation B (Right) containing isolated microbialite bioherms surrounded by skeletal grainstones (modified from Figure 19).* ***(d)*** *The model of Interpretation A (i.e., in (b) left) shows the 3D model created from sub-horizontal sketched surfaces. It is unknown when sketching if another surface will be truncated away from the current cross-section, so an operator is warranted.* ***(d)*** *The model of Interpretation B (i.e., in (b) right) shows the 3D model created from the same base model as for Interpretation A; the red top, base and central surfaces in both models are the same. To create Interpretation B, the top and central surfaces were selected. It is unknown when sketching if another surface will be truncated away from the current cross section, so an operator is warranted to preserve within that region (SR operator). The sketching plane was then moved up and down vertically, and circles were drawn in the plan view to create the conical geometries of the isolated bioherms.*

cause the circles on the upper plane are larger than the circles on the lower planes, the circles are interpolated to generate upward-widening conical mounds of the form interpreted by Bohacs *et al.* [BLWD*13]. This process is then repeated within a separate region to create a second stratigraphic level of microbialite bioherm mounds and grainstones.

7. Conclusions and future work

In this paper, we present a system that leverages algorithmic geologic operators for the conceptual SBIM of geologically consistent models built from stratigraphic surfaces. The operators are intuitive and flexible to domain experts, who successfully used them to create models at several length scales and depositional environments, from different data types. We also demonstrated that models created with our system honour fundamental, widely used stratigraphic and sedimentologic concepts such as the law of superposition, Walther's Law, sequence stratigraphy, and facies models (e.g., [WB99, JYMJ05, CCLCdV*09]).

Preliminary feedback from expert users on the use of our system is very positive, highlighting that the strength of our approach relative to current modelling tools lies in its intuitiveness, speed in generating models, flexibility, and practicality; surfaces can be sketched in any order to reflect different interpretations, or interpretations that evolve during sketching. Another benefit of our work is that it lays the foundations to formalizing the use of the operators in a way that easily allows for their incorporation in other modelling frameworks. Currently, our system is limited to generating models of stratigraphic surfaces and simple structural features (e.g. continuous fault surfaces and monotonic folded surfaces). In the future, we will extend this framework by allowing fault surfaces to terminate within geological domains (cf. Fig. 3(a), so faults can tip out within the modelled volume, and by allowing non-monotonic surfaces (e.g., recumbent folds) to be sketched and modelled. These geometric refinements will be supplemented with new operators that apply to structural and diagenetic surfaces and related heterogeneity. We will also conduct a formal user-study and evaluation on the SBIM interface and its functionality applied to different demonstration examples and case-studies. We designed RRM to include real-world data during the sketch-based modelling conceptualization. Our system currently supports seismic slices (as shown in the results). Support to other data sources is a work in progress.

Acknowledgments

This work was carried out by the Rapid Reservoir Modelling (RRM) Consortium. We would like to thank our sponsors, Equinor, ExxonMobil, Petrobras, Petronas, Shell, and IBM Research Brazil/IBM Centre for Advanced Studies (CAS) Alberta, Canada, for their support. We also thank the anonymous reviewers for their careful and valuable comments and suggestions.

References

[ABVB*12] AMORIM R., BOROUMAND N., VITAL BRAZIL E., HAJIZADEH Y., EATON D., COSTA SOUSA M.: Interactive sketch-based estimation of stimulated volume in unconventional reservoirs using microseismic data. In *13th European Conference on the Mathematics of Oil Recovery* (Biarritz, France, 09 2012), (ECMOR XIII), 11 pages. 3

[AOK12] ARISOY E., ORBAY G., KARA L.: Free form surface skinning of 3D curve clouds for conceptual shape design. *Journal of Computing and Information Science in Engineering 12*, 3 (09 2012), 031005 (13 pages). 2

[APCS09] ANASTACIO F., PRUSINKIEWICZ P., COSTA SOUSA M.: Sketch-based parameterization of L-systems using illustration-inspired construction lines and depth modulation. *Computers & Graphics 33*, 4 (2009), 440–451. 2

[AVBPCS12] AMORIM R., VITAL BRAZIL E., PATEL D., COSTA SOUSA M.: Sketch modeling of seismic horizons from uncertainty. In *9th International Symposium on Sketch-Based Interfaces and Modeling* (Annecy, France, 06 2012), (SBIM '12), pp. 1–10. 2, 3

[AVBSCS14] AMORIM R., VITAL BRAZIL E., SAMAVATI F., COSTA SOUSA M.: 3D geological modeling using sketches and annotations from geologic maps. In *11th International Symposium on Sketch-Based Interfaces and Modeling* (Vancouver, Canada, 08 2014), (SBIM '14), pp. 17–25. 3

[BBS08] BAE S.-H., BALAKRISHNAN R., SINGH K.: Ilovesketch: As-natural-as-possible sketching system for creating 3D curve models. In *21st Annual ACM Symposium on User Interface Software and Technology* (10 2008), pp. 151–160. 2

[BF04] BÁRDOSSYJÁNOS G., FODOR J.: *Evaluation of uncertainties and risks in geology*. Springer, 2004, ch. Review of the main uncertainties and risks in geology, pp. 3–12.

[BGSJ07] BOND C., GIBBS A., SHIPTON Z., JONES S.: What do you think this is? "conceptual uncertainty" in geoscience interpretation. *GSA Today 17* (11 2007), 4–10. 1

[BLWD*13] BOHACS K., LAMB-WOZNIAK K., DEMKO T., ELESON J., MCLAUGHLIN O., LASH C., CLEVELAND D., KACZMAREK S.: Vertical and lateral distribution of lacustrine carbonate lithofacies at the parasequence scale in the miocene hot spring limestone, idaho: An analog addressing reservoir presence and quality. *AAPG Bulletin 97*, 11 (2013), 1967–1995. 8, 10

[Can18] CANNON S.: *Reservoir Modelling: A Practical Guide*. John Wiley & Sons Ltd, 2018. 1

[CCLCdV*09] CAUMON G., COLLON P., LE CARLIER DE VESLUD C., VISEUR S., SAUSSE J.: Surface-based 3D modeling of geological structures. *Mathematical Geosciences 41* (11 2009), 927–945. 2, 5, 10

[Com17] COMPTON R. R.: *Geology in the Field*. CreateSpace Independent Publishing Platform, 2017. 1

[DPS15] DE PAOLI C., SINGH K.: SecondSkin: sketch-based construction of layered 3D models. *ACM Transactions on Graphics 34*, 4 (7 2015), 126:1–126:10. 2

[Duc77] DUCHON J.: Splines minimizing rotation-invariant semi-norms in Sobolev spaces. *Constructive Theory of Functions of Several Variables. Lecture Notes in Mathematics 571* (1977), 85–100. 7

[FNOV20] FERREIRA R. S., NOCE J., OLIVEIRA D. A. B., VITAL BRAZIL E.: Generating sketch-based synthetic seismic images with generative adversarial networks. *IEEE Geoscience and Remote Sensing Letters 17*, 8 (2020), 1460–1464. 3

[GCO*17] GARNIER B., CHANG M., ORMAND C., MATLEN B., TIKOFF B., SHIPLEY T. F.: Promoting sketching in introductory geoscience courses: CogSketch geoscience worksheets. *Topics in Cognitive Science (topiCS). Special Issue: Sketching and Cognition 9*, 4 (10 2017), 943–969. 1

[GCR*18] GARCIA M., CANI M.-P., RONFARD R., GOUT C., PERRENOUD C.: Automatic generation of geological stories from a single sketch. In *Joint Symposium on Computational Aesthetics and Sketch-Based Interfaces and Modeling and Non-Photorealistic Animation and Rendering* (2018), Expressive '18, pp. 1–15. 3

[GGP*19] GALIN E., GUÉRIN E., PEYTAVIE A., CORDONNIER G., CANI M.-P., BENES B., GAIN J.: A review of digital terrain modeling. *Computer Graphics Forum 38*, 2 (05 2019), 553–577. 2

[GJ12] GRIMM C., JOSHI P.: Just DrawIt: a 3D sketching system. In *9th International Symposium on Sketch-Based Interfaces and Modeling* (Annecy, France, 6 2012), (SBIM '12), p. 121–130. 2

[GUS*14] GENTNER D., UTTAL D., SAGEMAN B., MANDUCA C., ORMAND C., SHIPLEY T., TIKOFF B., EDUC R., MANDUCA C., ORMAND C., SHIPLEY T., JEE B.: Drawing on experience: how domain knowledge is reflected in sketches of scientific structures and processes. *Research in Science Education 44* (11 2014), 859–883. 1

[HCW16] HU X., CAI L., WANG Q.: Interactive and stochastic complex geological-surface reconstruction based on sketch. In *Society of Exploration Geophysicists International Exposition and 86th Annual Meeting (Expanded Abstracts)* (Dallas, USA, 10 2016), (SEG '16), pp. 1997–2002. 3

[Hod03] HODGES E. (Ed.): *The Guild Handbook of Scientific Illustration*. John Wiley and Sons, 2003. 1

[IYYI14] IJIRI T., YOSHIZAWA S., YOKOTA H., IGARASHI T.: Flower modeling via x-ray computed tomography. *ACM Transactions on Graphics 33*, 4 (07 2014), 1–10. 2

[JHR*15a] JACKSON M., HAMPSON G., ROOD D., GEIGER S., ZHANG Z., COSTA SOUSA M., AMORIM R., VITAL BRAZIL E., SAMAVATI F., GUIMARAES L.: Rapid Reservoir Modeling: prototyping of reservoir models, well trajectories and development options using an intuitive, sketch-based interface. In *SPE Reservoir Simulation Symposium* (Houston, USA, 02 2015), vol. 2 of *(SPE RSS '15)*, pp. 1–13. 3

[JHR*15b] JUNG A., HAHMANN S., ROHMER D., BEGAULT A., BOISSIEUX L., CANI M.-P.: Sketching folds: developable surfaces from non-planar silhouettes. *ACM Transactions on Graphics 34*, 5 (11 2015), 155:1–155:12. 2

[JHS*13] JACKSON M., HAMPSON G., SAUNDERS J., EL-SHEIKH A., GRAHAM G., MASSART B.: Surface-based reservoir modelling for flow simulation. *Geological Society, London, Special Publications 387* (06 2013), 271–292. 3

[JNHW13] JANOCKO M., NEMEC W., HENRIKSEN S., WARCHOŁ M.: The diversity of deep-water sinuous channel belts and slope valley-fill complexes. *Marine and Petroleum Geology 41* (2013), 7–34. Special Issue: Internal architecture, bedforms and geometry of turbidite channels. 4

[JS11] JORGE J., SAMAVATI F. (Eds.): *Sketch-based Interfaces and Modeling*. Springer, 2011. 2

[JYMJ05] JACKSON M. D., YOSHIDA S., MUGGERIDGE A. H., JOHNSON H. D.: Three-dimensional reservoir characterization and flow simulation of heterolithic tidal sandstones. *AAPG Bulletin 89*, 4 (2005), 507–528. 2, 5, 10

[LHV12] LIDAL E. M., HAUSER H., VIOLA I.: Geological storytelling: graphically exploring and communicating geological sketches. In *9th International Symposium on Sketch-Based Interfaces and Modeling* (Annecy, France, 06 2012), (SBIM '12), pp. 11–20. 3

[LNP*13] LIDAL E. M., NATALI M., PATEL D., HAUSER H., VIOLA I.: Geological storytelling. *Computers & Graphics 37*, 5 (2013), 445–459. 3

[LPB*13] LIDAL E., PATEL D., BENDIKSEN M., LANGELAND T., VIOLA I.: Rapid sketch-based 3D modeling of geology. In *Eurographics Workshop on Visualization in Environmental Sciences (Short Paper)* (Leipzig, Germany, 06 2013), (EnvirVis '13), pp. 1–5. 3

[LSC*19] LIU R., SHEN L., CHEN X., JI G., ZHAO B., TAN C., SU M.: Sketch-based slice interpretative visualization for stratigraphic data. *Journal of Imaging Science and Technology 63*, 6 (2019), 1–10. 3

[Mal02] MALLET J.-L.: *Reservoir Modelling: A Practical Guide*. Oxford University Press, 2002. 1

[MC06] MAYALL M. J. E., CASEY M.: Turbidite channel reservoirs—key elements in facies prediction and effective development. *Marine and Petroleum Geology 23*, 8 (09 2006), 821–841. 8

[MFS*20] MA H., FAN G., SHAO D., DING L., SUN H., ZHANG Y., ZHANG Y., CRONIN B.: Deep-water depositional architecture and sedimentary evolution in the rakhine basin, northeast bay of bengal. *Petroleum Science 17*, 3 (03 2020), 598–614. 2, 7, 8, 9

[MGR19] MOTTA S., GATTASS M., ROEHL D.: Sketch-based modeling of salt domes. In *SEG International Exposition and 89th Annual Meeting (Expanded Abstracts)* (San Antonio, TX, USA, 08 2019), (SEG '19), Society of Exploration Geophysicists (SEG), pp. 1828–1832. 3

[MMGR20] MOTTA S., MONTENEGRO A., GATTASS M., ROEHL D.: A 3D sketch-based formulation to model salt bodies from seismic data. *Computers & Geosciences 135*, 104457 (02 2020), 1–11. 3

[MPS*11] MCHARGUE T., PYRCZ M., SULLIVAN M., J.D. C., A. F., B.W. R., J.A. C., M. L., N.J. P. H. D.: Architecture of turbidite channel systems on the continental slope: Patterns and predictions. *Marine and Petroleum Geology 28*, 3 (03 2011), 728–743. 7, 8

[NHRT07] NILSSON B., HØJBERG A. L., REFSGAARD J. C., TROLDBORG L.: Uncertainty in geological and hydrogeological data. *Hydrology and Earth System Sciences 11* (2007), 1551–1561. 1

[NISA07] NEALEN A., IGARASHI T., SORKINE O., ALEXA M.: Fibermesh: designing freeform surfaces with 3D curves. *ACM Transactions on Graphics 26*, 3 (7 2007), 41:1–41:10.35. 2

[NKP14] NATALI M., KLAUSEN T. G., PATEL D.: Sketch-based modelling and visualization of geological deposition. *Computers & Geosciences 67C* (06 2014), 40–48. 3

[NLP*13] NATALI M., LIDAL E. M., PARULEK J., VIOLA I., PATEL D.: Modeling terrains and subsurface geology. In *Eurographics 2013 - State of the Art Reports (STARs)* (Girona, Spain, 05 2013), (EG '13), pp. 155–173. 2, 3

[NPP14] NATALI M., PARULEK J., PATEL D.: Rapid modelling of interactive geological illustrations with faults and compaction. In *30th Spring Conference on Computer Graphics* (Smolenice, Slovakia, 05 2014), (SCCG '14), p. 5–12. 3

[NVP12] NATALI M., VIOLA I., PATEL D.: Rapid visualization of geological concepts. In *XXV Conference on Graphics, Patterns and Images* (Ouro Preto, Brazil, 08 2012), (SIBGRAPI '12), pp. 150–157. 3

[OK12] ORBAY G., KARA L. B.: Sketch-based surface design using malleable curve networks. *Computers & Graphics 36*, 8 (12 2012), 916 – 929. 2

[OSCSJ09] OLSEN L., SAMAVATI F., COSTA SOUSA M., JORGE J.: Sketch-based modeling: a survey. *Computers & Graphics 33*, 1 (02 2009), 85–103. 2

[OSD06] OH J.-Y., STUERZLINGER W., DANAHY J.: SESAME: towards better 3D conceptual design systems. In *6th Conference on Designing Interactive Systems* (2006), (DIS '06), p. 80–89. 2

[PW09] PLATT N. H., WRIGHT V. P.: *Lacustrine Carbonates: Facies Models, Facies Distributions and Hydrocarbon Aspects*. John Wiley & Sons, Ltd, 2009, ch. 3, pp. 57–74. 8

[RBLM19] RANDLE C. H., BOND C. E., LARK R. M., MONAGHAN A. A.: Uncertainty in geological interpretations: Effectiveness of expert elicitations. *Geosphere 15*, 1 (01 2019), 108–118. 1

[Rob15] ROBERTSON S.: *How to Design: Concept Design Process, Styling, Inspiration, and Methodology*. Design Studio Press, 2015. 1

[SBSS12] SHAO C., BOUSSEAU A., SHEFFER A., SINGH K.: CrossShade: shading concept sketches using cross-section curves. *ACM Transactions on Graphics 31* (07 2012), 1–11. 2

[SHB09] SCHILD J., HOLTKÄMPER T., BOGEN M.: The 3D sketch slice: precise 3D volume annotations in virtual environments. In *15th Joint Virtual Reality Eurographics Conference on Virtual Environments* (Lyon, France, 2009), (JVRC '09), p. 65–72. 2

[SVBCS13] SULTANUM N., VITAL BRAZIL E., COSTA SOUSA M.: Navigating and annotating 3D geological outcrops through multi-touch interaction. In *ACM International Conference on Interactive Tabletops and Surfaces* (St. Andrews, UK, 10 2013), (ITS '13), p. 345–348. 3

[Vai87] VAIL P. R.: *AAPG Studies in Geology: Atlas of Seismic Stratigraphy*, vol. 1. American Association of Petroleum Geologists (AAPG), 1987, ch. Seismic stratigraphy interpretation using sequence stratigraphy: part 1: seismic stratigraphy interpretation procedure, pp. 1–10. 1

[VHFF15] VILLAMIZAR C., HAMPSON G., FLOOD Y., FITCH: Object-based modelling of avulsion-generated sandbody distributions and connectivity in a fluvial reservoir analogue of low to moderate net-to-gross ratio. *Petroleum Geoscience 21* (2015), 249–270. 2

[WB99] WHITE C., BARTON M.: Translating outcrop data to flow models, with applications to the ferron sandstone. *SPE Reservoir Evaluation and Engineering Journal 2*, 4 (08 1999), 341–350. 2, 5, 10

[WR05] WENDLAND H., RIEGER C.: Approximate interpolation with applications to selecting smoothing parameters. *Numerische Mathematik 101*, 4 (2005), 729–748. 7

[YCF10] YIN P., CHANG M., FORBUS K.: Sketch-based spatial reasoning in geologic interpretation. In *24th International Workshop on Qualitative Reasonin* (Portland, OR, USA, 08 2010), (QR2010), pp. 90–97. 1

[ZGR*17a] ZHANG Z., GEIGER S., ROOD M., JACQUEMYN C., JACKSON M., HAMPSON G., DE CARVALHO F., MACHADO SILVA C., MACHADO SILVA J., COSTA SOUSA M.: Flow diagnostics on fully unstructured grids. In *SPE Reservoir Simulation Conference* (Montgomery, TX, USA, 02 2017), (SPE RSC '17), 16 pages. 3, 4

[ZGR*17b] ZHANG Z., GEIGER S., ROOD M., JACQUEMYN C., JACKSON M., HAMPSON G., DE CARVALHO F., MACHADO SILVA C., MACHADO SILVA J., COSTA SOUSA M.: A tracing algorithm for flow diagnostics on fully unstructured grids with multipoint flux approximation. *SPE Journal 22* (2017), 1946–1962. 3, 4

[ZGR*18] ZHANG Z., GEIGER S., ROOD M., JACQUEMYN C., JACKSON M., HAMPSON G., DE CARVALHO F., MACHADO SILVA C., MACHADO SILVA J., COSTA SOUSA M.: Fast flow computation methods on unstructured tetrahedral meshes for rapid reservoir modelling. In *19th European Conference on the Mathematics of Oil Recovery* (Barcelona, Spain, 2018), (ECMOR XVI), pp. 1–15. 3, 4